Polymorphism, band-structure, band-lineup, and alloy energetics of the group II oxides and sulfides MgO, ZnO, CdO, MgS, ZnS, CdS

Stephan Lany*[a]

[a]National Renewable Energy Laboratory, 15013 Denver West Blvd, Golden, CO, USA 80401

ABSTRACT

The group II chalcogenides are an important class of functional semiconductor materials exhibiting a remarkable diversity in terms of structure and properties. In order to aid the materials design, a consistent set of electronic structure calculations is presented, including data on the polymorphic energy ordering, the band-structures, the band-lineups relative to the vacuum level, surface energies, as well as on the alloy energetics. To this end, current state-of-the-art electronic structure tools are employed, which, besides standard density functional theory (DFT), include total-energy calculation in the random phase approximation and GW quasiparticle energy calculations. The ionization potentials and electron affinities are obtained by combining the results of bulk GW and surface DFT calculations. Considering both octahedral and tetrahedral coordination symmetries, exemplified by the rock-salt and zinc-blende lattices, respectively, this data reveals both the chemical and structural trends within this materials family.

Keywords: Transparent conducting oxides, functional materials, polymorphism, band-structure, ionization potential, semiconductor alloys, mixing enthalpy, surface energies

*Stephan.Lany@NREL.gov

1. INTRODUCTION

Despite their chemical similarity, the group II chalcogenides (here, oxides and sulfides of Mg, Zn, Cd) represent a remarkably diverse group of semiconducting and insulating materials. Structurally, it contains both octahedral (rocksalt MgO, CdO, MgS) and tetrahedral (zinc-blende or wurtzite ZnO, ZnS, CdS) motifs; electronically, it contains large and small gap systems like (MgO and CdO, respectively) with both direct and indirect characters (particularly, CdO is strongly indirect). In regards of their opto-electronic functionality, ZnO is notable as a transparent conducting oxide [1], and CdS as buffer layer in thin-film solar cells [2]. Recently, alloys of group II chalcogenides are receiving increased interest as tailored functional materials, including mixed metal alloys like ZnMgO and CdZnO [3][4], CdZnS [5], as well as mixed anion systems like ZnOS [6]. Given the polymorphic nature of the II chalcogenide family, it is therefore interesting to evaluate systematically both the structure dependence of the properties and the alloy energetics, so to form a basis for establishing "design principles" as to which alloys can be formed in which structure with which properties. Previous theoretical work has predicted band-structure and optical properties for the II oxides [12], and there exists a

Oxide-based Materials and Devices V, edited by Ferechteh H. Teherani, David C. Look, David J. Rogers, Proc. of SPIE Vol. 8987, 89870K · © 2014 SPIE
CCC code: 0277-786X/14/$18 · doi: 10.1117/12.2043587

body of literature on the polymorphism of binary compounds [7] [8] [9] [10] [11] and the properties of individual alloy systems [3][4][5][6]. In the present work, state-of-the-art electronic structure tools are used to map out a wider range of compositions and properties, thereby providing a consistent dataset for the oxides and sulfides of Mg, Zn, and Cd in regard of the polymorph energies, band-structures, band-lineups (ionization potentials and electron affinities), and alloy energetics, including the respective composition ranges where the octahedral and tetrahedral structures are expected to be stable.

1.1 Methods

The present work utilizes several electronic structure tools, which are implemented within the projector augmented wave (PAW) framework in the VASP code: (i) Density functional theory (DFT) calculations using the generalized gradient approximation (GGA) [13][14]. (ii) Total energy calculations within the random phase approximation (RPA) based on the adiabatic connection dissipation fluctuation theorem [15][16]. (iii) GW quasiparticle energy calculations [17][18]. The polymorph energies are determined for the rocksalt (RS), zincblende (ZB), and wurtzite (WZ) structures using the RPA, which has recently been shown to provide an improved description of polymorphic energy ordering compared to standard DFT [19]. Since the ZB and WZ polymorphs have rather similar energies and properties, the RS and ZB structures are used as prototypes for the octahedral and tetrahedral coordination symmetries. The respective band-structures are calculated in GW, following the same general recipe that has been published before [20][21], i.e., maintaining the DFT wavefunctions, but iterating the eigenenergies to self-consistency. Brillouin zone sampling was performed on a Γ centered 12×12×12 k-mesh. In order to improve the *d*-orbital energies, which tend to be overestimated in GW [22], an additional on-site potential for Zn-*d* (V_d = –1.5 eV) and Cd-*d* (V_d = –0.5 eV) is applied in the GW calculation, as described previously [23]. For both the RPA and the GW calculations, the GGA+U [24] method is used (U_{Zn} = 6 eV, U_{Cd} = 5 eV) to generate the wavefunctions on which the total and quasiparticle energies are evaluated. Following the rationale for combining DFT and GW results as recently established for defect [25] and surface calculations [26], the potential step at the nonpolar (100) and (110) surfaces of the RS and ZB structures is calculated in DFT with the same functional as used for generating the wavefunctions for the GW calculations, so that the GW quasiparticle energies can be directly referred to the vacuum level. The typical overestimation of the lattice constant by about 1% in GGA has been accounted for by a scaling of the lattice volume prior to the calculations of the surface potential step and the quasi-particle energies. Finally, the alloy mixing enthalpies are determined by using the polymorph energies from RPA, and random alloy models, calculated in GGA using the special quasi-random structures (SQS) of Ref. [27] for both the RS and ZB lattices.

2. RESULTS AND DISCUSSION

2.1 Polymorphism

The polymorphic energy ordering of the II chalcogenides has been calculated on the DFT level in the previous literature [7][9]. In a recent study [19], we have shown that the RPA is able to overcome the difficulty of various DFT functionals to describe the energy ordering in the transition metal oxide MnO [28]. Less dramatic, but nevertheless significant differences between DFT and RPA were also observed for MgO and ZnO. Thus, the energy ordering of the II chalcogenides is reevaluated in the present work using the RPA, and the results are summarized in table 1. Besides an increase of the bulk modulus by about 20% and a reduction of the lattice volume by about 3% (which improves the agreement of the lattice constants with experiment), the most important change due to the RPA is the relative stabilization of the octahedral (RS) over the tetrahedral (ZB and WZ) coordination: The energy difference $[E_{RPA}(RS) - E_{RPA}(ZB)] - [E_{DFT}(RS) - E_{DFT}(ZB)]$ ranges from –31 meV for ZnS to as much as –139 meV for CdS. The energy difference between the two tetrahedral polymorphs (ZB and WZ) is comparatively small, both in DFT and RPA, as expected. Notably, the RPA predicts that the ZB structure of CdS is slightly lower in energy than the WZ phase, which is generally considered to be the ground state [29], even though the zinc-blende modification of CdS is well known. However, the energy difference of 8 meV/fu is small enough to be considered essentially degenerate within the limits of the calculations, which do not include zero point motion and finite temperature effects. Note that MgO is not stable in the WZ structure [11], and is therefore omitted in table 1. Due to the small energy difference between ZB and WZ, and the generally rather similar properties of the II chalcogenides in these structures, the ZB polymorph is taken as a prototype for the tetrahedral modification in the following. Table 1 reveals a number of polymorph/substrate combinations that are lattice matched and could interesting for the study of polymorphism in epitaxial growth: ZB-MgO/CdO, ZB-ZnO/CdO, ZB-CdO/MgS, RS-ZnS/MgS (note, however, the exceptionally high energy of RS-ZnS), RS-CdS/ZnS.

Table 1. Polymorphism of group II chalcogenides. The DFT (GGA) and RPA energies are given with respect to the ground state structure (bold). The bulk moduli (B_0) and lattice volumes V per formula unit (fu) are given are also given for the RPA.

	Structure	ΔE_{GGA} (meV)	ΔE_{RPA} (meV)	B_0 (GPa)	V (Å^3/fu)
MgO	**RS**	0	0	172	18.87
	ZB	214	297	128	24.10
ZnO	RS	304	239	183	19.90
	ZB	15	20	157	24.21
	WZ	0	0	156	24.26
CdO	**RS**	0	0	186	26.05
	ZB	31	95	86	33.66
	WZ	8	119	108	33.08
MgS	**RS**	0	0	90	34.54
	ZB	30	88	63	44.79
ZnS	RS	640	610	105	32.59
	ZB	0	0	81	39.30
	WZ	4	13	82	39.22
CdS	RS	278	127	93	40.09
	ZB	4	-8	68	50.28
	WZ	0	0	66	50.37

2.2 Band-structure and band lineup

With exception of MgS, the band-structure properties of the II chalcogenides in their ground state structure are fairly well established [30]. The direct band gap of CdO has been studied in detail recently [31], but the indirect band gap is not well known experimentally. Theoretically, state-of-the-art GW band-structure calculations have been reported mostly for most of the II chalcogenides [12] [22], and some band-structure predictions exist for polymorphism [7][11][32]. The purpose of the present work is to provide a comprehensive comparison between oxides and sulfides, and between the RS and ZB polymorphs, based on a consistent set of data calculated by the same approach. In addition, the combination of GW bulk and DFT surface calculations allows for a quantitative prediction of the band-lineups with respect to the vacuum level at the non-polar (100) and (110) surfaces of the RS and ZB structures, respectively. The results are summarized in table 2, and the band-structures are plotted in figure 1. We observe the following trends: (i) ZB compounds are all direct semiconductors with a band gap at the Brillouin zone center. (ii) In the RS structure, the IIb chalcogenides have the valence band maximum (VBM) at the L point, which can be traced back to the fact that in the octahedral symmetry, the *p-d* repulsion is forbidden at the Γ point, but allowed at the L point [33]. For example, the calculated direct gap of CdO is 2.0 eV, whereas the indirect gap is only 0.9 eV (see table 2). Note that the Zn and Cd sulfides in the RS structure have valence band energies inside the Brillouin zone that are essentially degenerate with the L point. (iii) The RS sulfides have indirect gaps with the conduction band minimum (CBM) at the X point. (iv) The IPs of the ZB structures are about 1 eV larger that those in the RS structure. (v) The IPs do not show the same chemical trends with the anion type as observed in band-offset calculations [34]: The sulfides have similar or even larger IPs than the oxides, i.e., a lower VBM energy. The present predictions agree rather well with experimental values for ZnO, ZnS, and CdS, where the IPs have been determined as 7.8, 7.5, and 7.3 [35]. However, one should consider that the IP are often sensitive to the surface orientation and termination [26][36]. The difference in the trends between band-offsets and IP is notable, in particular since the band offsets were constructed to eliminate strain effects that inevitably occur at the coherent epitaxial interface in a slab supercell (in contrast, there is no strain at the free surface used to calculate the IP). However, the construction of such a ”natural band offset” [37] relies of the definition of a potential reference, which introduces some ambiguity [38][39]. Further insight, as to whether the band offset in lattice-mismatched non-epitaxial interfaces is controlled by the natural band-offsets or the difference in IPs, is desirable.

Table 2. The predicted ionization potentials (IP), electron affinities (EA), band-gaps (E_g), and surface energies (E_{surf}) of II chalcogenides. The IP, EA, and E_{surf} are for the (100) and (110) surfaces of the RS and ZB structures, respectively, and the direct (*d*) or indirect (*i*) character of the band gap is indicated.

Cation	Structure	Oxides				Sulfides			
		IP (eV)	EA (eV)	E_g (eV)	E_{surf} (meV/Å^2)	IP (eV)	EA (eV)	E_g (eV)	E_{surf} (eV/Å^2)
Mg	RS	7.14	–1.04	8.17 *d*	55.79	6.91	2.11	4.80 *i*	25.20
	ZB	8.02	1.28	6.74 *d*	82.51	8.29	2.63	5.66 *d*	35.77
Zn	RS	6.35	2.95	3.40 *i*	36.80	6.29	5.00	1.29 *i*	14.46
	ZB	7.34	4.13	3.22 *d*	55.81	7.49	3.46	4.03 *d*	25.98
Cd	RS	5.23	4.36	0.87 *i*	34.20	6.08	4.31	1.77 *i*	17.20
	ZB	6.10	5.29	0.81 *d*	43.85	7.11	4.40	2.71 *d*	22.05

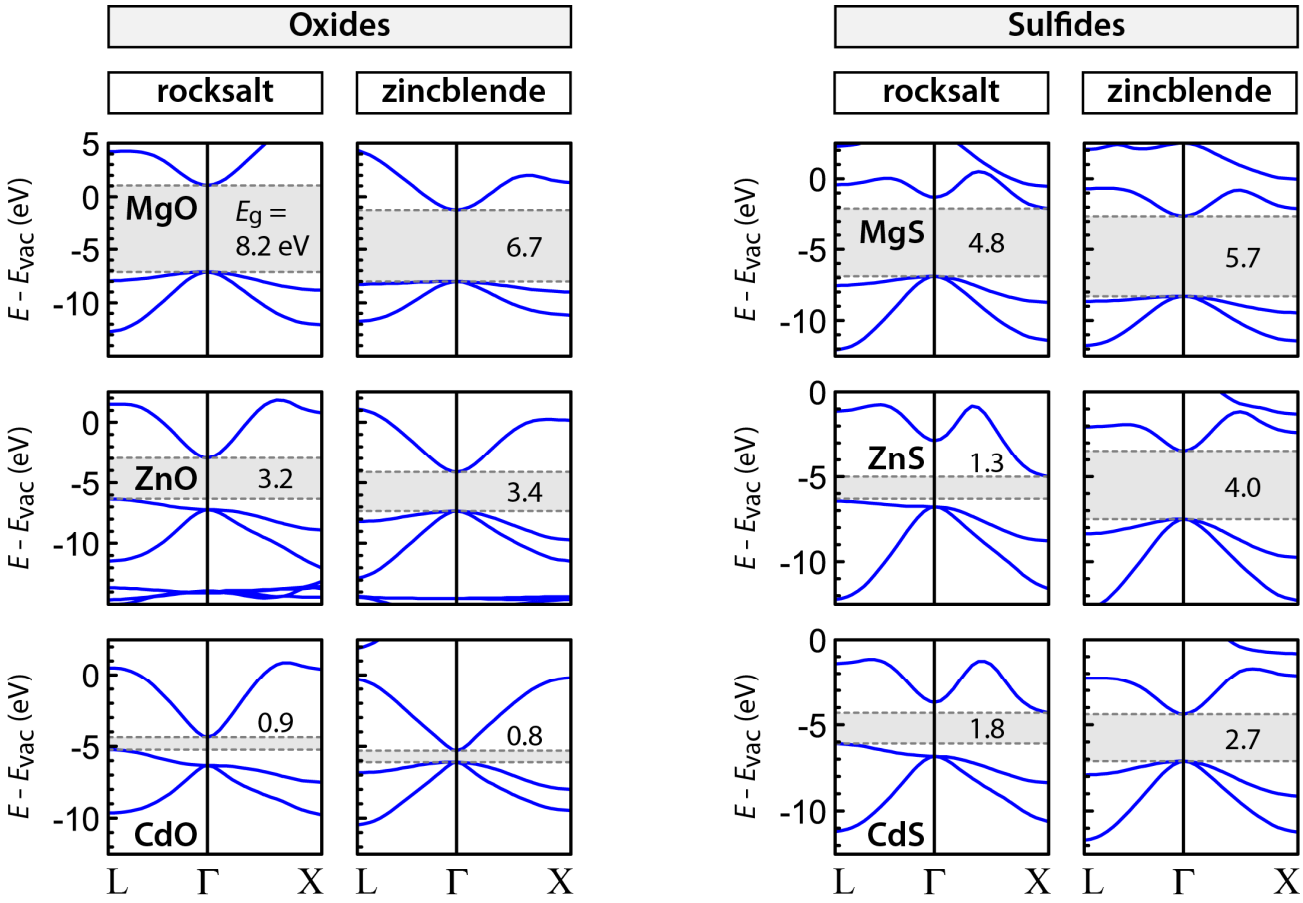

Figure 1. Band-structure energies calculated in the GW approximation for the group II oxides and sulfides. The energy zero is the vacuum level at the (100) surface of the rocksalt structure and at the (110) surface of the zincblende structure.

Shown in Table 2 are also the calculated surface energies (E_{surf}) for the (100) and (110) surfaces of the Rs and ZB structures, respectively. The chemical trends are that oxides have a larger E_{surf} than sulfides, and that E_{surf} decreases along the cation series Mg $\rightarrow$ Zn $\rightarrow$ Cd. The structural trend is that RS surfaces have a lower energy than ZB surfaces.

2.3 Alloy mixing enthalpies

In many alloy systems, the mixing enthalpies are well described to quadratic order by a single alloy interaction parameter Ω [40], which implies that the mixing enthalpy of an $A_{1-x}B_x$ alloy, $\Delta H_m(x) = E(A_{1-x}B_x) - (1-x)\cdot E(A) - x\cdot E(B)$, is symmetric with respect to $x = 0.5$. Including the possibility of an asymmetric mixing enthalpy, and considering that we are dealing here with alloys between heterostructural end compounds, the mixing enthalpy can be expressed up to 3rd order as

$$\Delta H_m(x) = (1-x)E_0 + xE_1 + \Omega x(1-x) + \Omega'(x^2 - x)(x - 0.5). \quad (1)$$

Here, E_0 and E_1 are the energies of the end compounds relative to the ground state structure, Ω is the regular alloy interaction parameter, and Ω' is the 3rd order parameter describing the asymmetry of ΔH_m. Using the DFT (GGA) energies of SQS alloy models for $x = 0.25$, 0.5, 0.75, and taking E_0 and E_1 as the RPA energy differences between the respective RS and ZB structures (see table 1), the Ω and Ω' parameters were fitted as shown in table 3. The full $\Delta H_m(x)$ diagrams are shown in figure 2.

Table 3. The alloy interaction parameters Ω and Ω', fitted according to eq. (1), for both the RS and ZB structures.

Alloy	Ω_{RS} (eV)	$\Omega' c_{RS}$ (eV)	Ω_{ZB} (eV)	Ω'_{ZB} (eV)
$Mg_{1-x}Zn_xO$	–0.04	–0.02	–0.08	–0.01
$Mg_{1-x}Cd_xO$	+0.69	+0.37	+0.06	–0.06
$Zn_{1-x}Cd_xO$	+0.43	+0.09	+0.15	–0.01
$Mg_{1-x}Zn_xS$	+0.08	+0.01	+0.07	±0.00
$Mg_{1-x}Cd_xS$	+0.17	+0.04	+0.01	–0.01
$Zn_{1-x}Cd_xS$	+0.21	±0.00	+0.12	±0.00
$MgO_{1-x}S_x$	+1.80	+1.20	+0.79	+0.03
$ZnO_{1-x}S$	+0.79	+0.82	+0.59	+0.06
$CdO_{1-x}S$	+0.61	+0.37	+0.32	–0.06

A number of observations can be made about the alloy interaction parameters: (i) In the RS structure, the mixing enthalpies are larger (Ω) and more asymmetric (Ω') than in the ZB structure. This behavior is likely related to the much higher density of the RS structure (see table 1). In the more open structure of the ZB lattice, strain due to atomic size mismatch is more easily relieved at a lower energy cost. In cases with strong asymmetries, the signs of Ω' are positive, indicating that it costs more energy to substitute a large atom for a small atom than vice versa. This behavior can be expected from the asymmetry of atomic pair potentials, where the energy rises more quickly for a distance reduction relative to the energy minimum than for an increase [41]. (ii) The alloy interaction parameters are larger in the mixed anion alloys than in the mixed cation alloys, reflecting the larger size mismatch between O and S, as compared to that between the Mg, Zn, and Cd (*cf.* the lattice volumes in table 1). (iii) The small values of Ω for the Mg/Zn alloys reflect their small size mismatch. In these cases, the mixing enthalpy is dominated by the polymorphic energy difference. As seen in figure 2, composition dependent structure transitions are expected for $Mg_{1-x}Zn_xO$, $Zn_{1-x}Cd_xO$, $Mg_{1-x}Zn_xS$, $Mg_{1-x}Cd_xS$, $MgO_{1-x}S_x$, and $CdO_{1-x}S_x$. For $Mg_{1-x}Zn_xO$ and $Zn_{1-x}Cd_xO$, these transitions have been observed experimentally at similar compositions [4][42]. Note that the DFT values for the polymorph energies of CdO and ZnO (table 1) would imply a minute stability range of the RS structure in $Zn_{1-x}Cd_xO$ alloys in the Cd rich regime, whereas experiments indicate a stability range $0.7 < x \leq 1.0$ that is even wider than predicted from the RPA results. This observation further corroborates the finding that DFT (GGA) overly favors the tetrahedral symmetry. An interesting situation is found for $MgO_{1-x}S_x$, where the end compounds have the RS structure, but due to the smaller value of Ω_{ZB}, the ZB structure is predicted to be stable within the composition interval $0.25 < x < 0.73$.

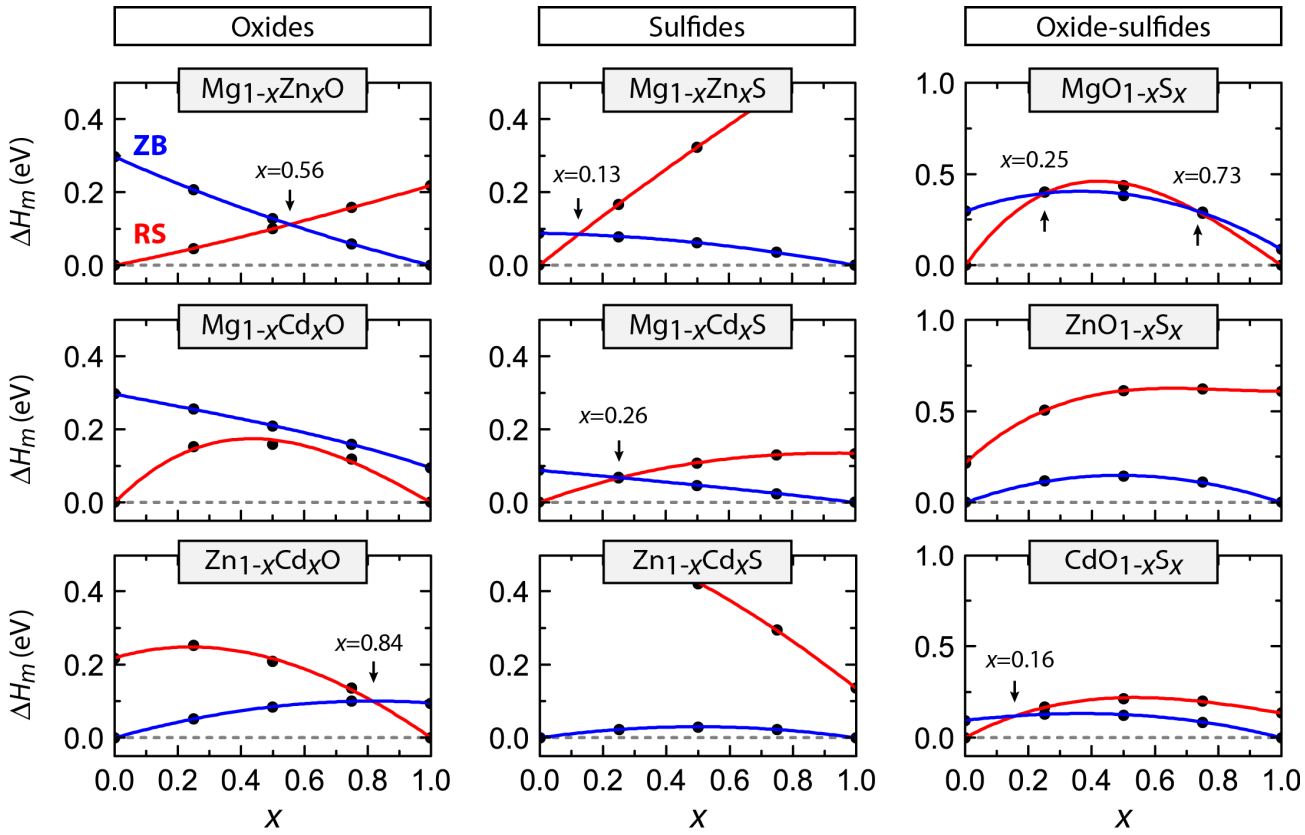

Figure 2. Calculated alloy mixing enthalpies ΔH_m for both the octahedral RS and the tetrahedral ZB lattices. The data points are obtained from the RPA polymorph energies (see table 1) and the DFT mixing enthalpies within the RS/ZB lattices for SQS cells at compositions x = 0.25, 0.5, and 0.75. The lines show the results of the fitting according to eq. (1). Note the difference energy scale for oxide-sulfide alloys.

3. CONCLUSIONS

The polymorphism, band-structures, band-lineups relative to the vacuum level, and alloy mixing enthalpies have been calculated for the oxides and sulfides of Mg, Zn, and Cd. By providing a comprehensive and consistent dataset for this materials family, these results should serve as reference data for the design of functional materials, such as transparent conductors, contacts, or heterojunction partners, e.g., for earth abundant photovoltaic materials. A number of lattice matched polymorph/substrate combinations were identified that could be interesting for study of polymorphism in epitaxial growth. The band-lineup calculations revealed that the ionization potentials in the tetrahedral ZB structure are about 1 eV larger than in the respective octahedral RS structure of the same compound. Notably, the IPs do not exhibit the same chemical trends with the anion type as expected from band offset calculations, a difference that is likely related to the absence of epitaxial strain at the free surface. The alloy mixing enthalpies exhibit in several cases a change of the energy ordering between the RS and ZB structures at certain critical compositions. For $MgO_{1-x}S_x$, there exists a composition interval within which the ZB is found to be lower in energy than the RS structure, even though RS is the ground state of both MgO and MgS.

ACKNOWLEDGEMENTS

This work was supported by the US Department of Energy, Office of Science, Office of Basic Energy Sciences, as part of an Energy Frontier Research Center under contract No. DE-AC36-08GO28308 to NREL. This work utilized high

performance computing resources sponsored by the Department of Energy's Office of Energy Efficiency and Renewable Energy, located at NREL.

REFERENCES

[1] Ozgur, U., Alivov, Y.I., Liu, C., Teke, A., Reshchikov, M.A., Doan, S., Avrutin, V., Cho, S.-J., and Morkoc, H., "A comprehensive review of ZnO materials and devices," J. Appl. Phys. 98, 041301 (2005).

[2] Rau U. and Schock H.W., "Cu(In,Ga)Se_2 Solar Cells," In: [Photoconversion of Solar Energy, 1: Clean Electricity From Photovoltaics], Archer, M.D. and Hill, R. (eds), Imperial College Press, London, 300-301 (2001).

[3] Makino, T., Segawa, Y., Kawasaki, M. , Ohtomo, A., Shiroki, R., Tamura, K., Yasuda, T., and Koinuma, H., "Band gap engineering based on $Mg_xZn_{1-x}O$ and $Cd_yZn_{1-y}O$ ternary alloy films," Appl. Phys. Lett. 78 , 1237 (2001).

[4] Detert, D.M., Lim, S.,H.,M., Tom, K., Luce, A.V., Anders, A., Dubon, O.D., Yu, K.M., and Walukiewicz, W., "Crystal structure and properties of $Cd_xZn_{1-x}O$ alloys across the full composition range," Applied Physics Letters 102, 232103 (2013).

[5] Bhattacharya, R.N., Contreras, M.A., Egaas, B., Noufi, R.N., Kanevce, A., and Sites, J.R., "High efficiency thin-film $CuIn_{1-x}Ga_xSe_2$ photovoltaic cells using a $Cd_{1-x}Zn_xS$ buffer layer," Appl. Phys. Lett. 89, 253503 (2006).

[6] Sun, L., Haight, R., Sinsermsuksakul, P., Kim, S.B., Park, H.H., and Gordon, R.G., "Band alignment of SnS/Zn(O,S) heterojunctions in SnS thin film solar cells," Appl. Phys. Lett. 103, 181904 (2013).

[7] Schleife, A., Fuchs, F., Furthmuller, J., and Bechstedt, F., "First-principles study of ground- and excited-state properties of MgO, ZnO, and CdO polymorphs," Phys. Rev. B 73, 245212 (2006).

[8] Ashrafia, A., and Jagadish, C., "Review of zincblende ZnO: Stability of metastable ZnO phases," J. Appl. Phys. 102, 071101 (2007).

[9] Sangthong, W., Limtrakul, J., Illas, F., and Bromley, S.T., "Predicting transition pressures for obtaining nanoporous semiconductor polymorphs: oxides and chalcogenides of Zn, Cd and Mg," Phys. Chem. Chem. Phys. 12, 8513 (2010).

[10] Rajan, A., Moug, R.T., and Prior, K.A., "Growth and stability of zinc blende MgS on GaAs, GaP, and InP substrates," Appl. Phys. Lett. 102, 032102 (2013).

[11] Limpijumnong, S., and Lambrecht, W.R.L. "Theoretical study of the relative stability of wurtzite and rocksalt phases in MgO and GaN," Phys. Rev. B 63, 104103 (2001).

[12] Schleife, A., Rodl, C., Fuchs, F., Furthmuuller, J., and Bechstedt, F., "Optical and energy-loss spectra of MgO, ZnO, and CdO from ab initio many-body calculations," Phys. Rev. B 80, 035112 (2009).

[13] Kresse, G., Joubert, D., "From ultrasoft pseudopotentials to the projector augmented-wave method," Phys. Rev. B 59, 1758 (1999).

[14] Perdew, J.P., Burke, K., and Ernzerhof, M., "Generalized Gradient Approximation Made Simple," Phys. Rev. Lett. 77, 3865 (1996).

[15] Langreth, D.C., and Perdew, J.P., "Exchange-correlation energy of a metallic surface: Wave-vector analysis," Phys. Rev. B 15, 2884 (1977).

[16] Harl, J., Schimka, L., and Kresse, G., "Assessing the quality of the random phase approximation for lattice constants and atomization energies of solids," Phys. Rev. B 81, 115126 (2010).

[17] Hedin, L., "New method for calculating the one-particle Green's function with application to the electron-gas problem," Phys. Rev. 139, A796 (1965).

[18] Shishkin, M., and Kresse, G., "Implementation and performance of the frequency-dependent GW method within the PAW framework," Phys. Rev. B 74, 035101 (2006).

[19] Peng, H., and Lany, S., "Polymorphic energy ordering of MgO, ZnO, GaN, and MnO within the random phase approximation," Phys. Rev. B 87, 174113 (2013).

[20] Peng, H., and Lany, S., "Semiconducting transition-metal oxides based on **d**5 cations: Theory for MnO and Fe_2O_3," Phys. Rev. B 85, 201202(R) (2012).

[21] Lany, S., "Band-structure calculations for the 3d transition metal oxides in GW," Phys. Rev. B 87, 085112 (2013).

[22] Shishkin, M., Marsman, M., and Kresse, G., "Accurate Quasiparticle Spectra from Self-Consistent GW Calculations with Vertex Corrections," Phys. Rev. Lett. 99, 246403 (2007).

[23] Lim, L.Y., Lany, S., Chang, Y.J., Rotenberg, E., Zunger, A., and Toney, M.F., "Angle-resolved photoemission and quasiparticle calculation of ZnO: The need for d band shift in oxide semiconductors," Phys. Rev. B 86, 235113 (2012).

[24] Dudarev, S.L., Botton, G.A., Savrasov, S.Y., Humphreys, C.J., and Sutton, A.P., "Electron-energy-loss spectra and the structural stability of nickel oxide: An LSDA+U study," Phys. Rev. B 57, 1505 (1998).
[25] Peng, H., Scanlon, D.O., Stevanovic, V., Vidal, J., Watson, G.W., and Lany, S., "Convergence of density and hybrid functional defect calculations for compound semiconductors," Phys. Rev. B 88, 115201 (2013).
[26] Stevanovic, V., Lany, S., Ginley, D.S., Tumas, W., and Zunger, A., "Assessing capability of semiconductors to split water using ionization potentials and electron affinities only," Phys. Chem. Chem. Phys. 16, 3706 (2014).
[27] Wei, S.-H., Ferreira, L.G., Bernard, J.E., and Zunger, A., "Electronic properties of random alloys: Special quasirandom structures, " Phys. Rev. B 42, 9622 (1990).
[28] Schron, A., Rodl, C., and Bechstedt, F., "Energetic stability and magnetic properties of MnO in the rocksalt, wurtzite, and zinc-blende structures: Influence of exchange and correlation," Phys. Rev. B 82, 165109 (2010).
[29] Rittner, E. S., Schulman, J. H., "Studies on the Coprecipitation of Cadmium and Mercuric Sulfides," J. Phys. Chem. 47, 537 (1943).
[30] Madelung, O., Rossler, U., Schulz, M., (ed.), [SpringerMaterials - The Landolt-Bornstein Database] http://www.springermaterials.com.
[31] Vasheghani Farahani, S.K., Munoz-Sanjose, V., Zuniga-Perez, J., McConville, C.F., and Veal, T.D., "Temperature dependence of the direct bandgap and transport properties of CdO," Appl. Phys. Lett. 102, 022102 (2013).
[32] Yan, Q., Rinke, P., Winkelnkemper, M., Qteish, A., Bimberg, D., Scheffler, M., and van de Walle, C.G., "Strain effects and band parameters in MgO, ZnO, and CdO," Appl. Phys. Lett. 101, 152105 (2012).
[33] Jaffe, J.E., Pandey, R., Kunz, A.B., "Electronic structure of rocksalt-structure semiconductors ZnO and CdO," Phys. Rev. B 43, 14030 (1991).
[34] Wei, S.-H., and Zunger, A., "Calculated natural band offsets of all II–VI and III–V semiconductors: Chemical trends and the role of cation *d* orbitals," Applied Physics Letters 72 , 2011 (1998).
[35] Swank, R.K., "Surface properties of II-VI compounds," Phys. Rev. 153, 844 (1967).
[36] Klein, A., Korber, C, Wachau, A. Sauberlich, F., Gassenbauer, Y., Schafranek, R., Harvey, S.P., and, Mason, T.O., "Surface potentials of magnetron sputtered transparent conducting oxides," Thin Solid Films 518, 1197 (2009).
[37] Shih, C.K., and Spicer, W.E., "Determination of a natural band-offset: The case of HgTe and CdTe," Phys. Rev. Lett. 58, 2594 (1987).
[38] van de Walle, C.G., and Martin, R.M., "Theoretical study of band offsets at semiconductor interfaces," Phys. Rev. B 35, 8154 (1987).
[39] Lany, S., Osorio-Guillen, J., and Zunger, A., "Origins of the doping asymmetry in oxides: Hole doping in NiO versus electron doping in ZnO," Phys. Rev. B 75, 241203(R) (2007).
[40] Stringfellow, G.B., [Organometallic Vapor-phase Expitaxy: Theory and Practice], Academic Press, New York, (1989).
[41] Lennard-Jones, J. E., "Cohesion," Proceedings of the Physical Society 43, 461 (1931).
[42] Chen, N.B., and, Sui, C.H., "Recent progress in research on $Mg_xZn_{1-x}O$ alloys," Materials Science and Engineering B 126, 16 (2006).